A Tapping-Mode AFM Study of the Compression of Grafted Poly(ethylene glycol) Chains

Ijeoma M. Nnebe and James W. Schneider*

Department of Chemical Engineering, Carnegie Mellon University, Pittsburgh, Pennsylvania 15213-3890

Received January 8, 2005; Revised Manuscript Received February 17, 2006

ABSTRACT: We investigate the measurement of forces arising from the compression of surface-grafted poly(ethylene glycol), PEG, chains in aqueous solutions using sharp, unmodified tips in Tapping-Mode atomic force microscopy (TM-AFM). PEG chains were grafted to silica by reaction with preadsorbed poly(ethylenimine) (PEI), affording control of grafting density by reaction conditions. Numerical simulation of the cantilever oscillation, accounting for distance-dependent damping, was used to quantify the effective forces measured in TM-AFM. The decay length of the steric force was compared to those obtained using conventional AFM, and a good correlation was found between the two methods using PEG chains in both a mushroom and brush conformation. A significant disparity in the magnitude of the steric force obtained by conventional AFM force measurements and TM-AFM was observed, and this was attributed to a deeper compression/penetration of the polymer-coated surface by the tip in the case of TM-AFM.

Introduction

Steric stabilization forces exerted by polymers at interfaces are crucial to many industrial processes. Atomic force microscopy (AFM) has been used extensively to study the interfacial properties of both adsorbed and grafted polymer layers.[1−4] Specifically, the use of colloidal spheres as probes has enabled AFM measurements to be compared to theory.[1,5−8] These colloidal probe AFM measurements have validated many theories developed to describe the behavior of polymer chains at the solid−liquid interface. Microspheres used as probes can range from 3 to 100 μm in diameter,[1,8,9] with the lower limit set essentially by the attachment procedure.

One disadvantage of the use of colloidal probes is that interactions arising from a small number of molecules cannot be distinguished. Local variations in interfacial properties of polymer layers may arise from incomplete surface coverage, polydispersity of chain lengths, and adsorption of material from solution, whether desirable or undesirable. Local force measurements require high lateral resolution that is achieved through the use of sharpened, integrated tips that are available with most AFM cantilevers. These tips have apex radii of curvature (R) between 5 and 30 nm, and though their complex geometry complicates theoretical comparison with experimental data, to a rough approximation, the tip apex can be treated as hemispherical for data reduction purposes.

In standard (contact mode or DC) AFM force measurements with sharp tips, however, unusual polymer chain dynamics have been reported. Kelley et al.[2] observed shallower steric force profiles, as compared with surface forces apparatus (SFA) data, in force measurements on poly(2-vinylpyridine)−polystyrene (PVP−PS) brushes using Si_3N_4 AFM tips ($R = 40$ nm). Their work appears to support earlier simulation work by Murat and Grest,[9] who showed that polymer segments readily escape away from a compressing AFM tip due to the finite size of the tip resulting in a slow resistance to compression. Guffond, William, and Sevick[10] provide insight into the origins of the escape transition of polymer chains and have shown that in Θ solvents polymer chains escape compression from finite-sized objects to minimize their free energy once the compression energy starts to get very large. The probability of escape is affected by the alignment of the compressing object over the chain and the ratio of the energy penalty associated with compression vs the penalty associated with stretching the chain to enable escape.

While not always in operation, the possibility of chain escape certainly confounds the interpretation of force data collected using sharp tips. In this report, we explore the use of force curves collected using sharp tips in Tapping-Mode (TM) AFM. TM-AFM measures, either directly or indirectly, small changes in the resonant frequency of the cantilever that result from tip−sample interactions. Various modeling methods exist to obtain the tip−sample interaction from these frequency shifts.[11] Broadly, there are two means of collecting force data using TM-AFM. One is to excite the base of the cantilever at a constant drive amplitude and measure the decrease in tip amplitude changes as the sample approaches. This "constant excitation" method can be applied to most commercial AFM systems without modification. A complication is that amplitude attenuation results from both resonant frequency shifts and broadening of the cantilever resonance brought on the increased damping of the cantilever oscillation during sample approach. As such, the method has been applied chiefly in dry systems where damping can be neglected. Our recent work[12] has shown that distance-dependent damping effects can be accounted for in liquid systems by tracking the quality of cantilever resonance, not phase shifts, during the measurement. This is accomplished by sampling the deflection data at high rates and performing a spectral analysis of the streamed deflection data. In so doing, TM-AFM data obtained from commercial instruments can be used without incorporating phase data that can be confounded by the presence of spurious resonances and external losses. It should be noted the observed quality of cantilever resonance may also be impacted by spurious resonances and external losses, but these cases are readily distinguished by the shape of the resonance peak obtained.

Alternative approaches circumvent these uncertainties by using custom AFM configurations. A method developed by

* To whom correspondence should be addressed.

10.1021/ma050045q CCC: $33.50
Published on Web 04/13/2006

Sader and co-workers[13] drive the AFM cantilever using magnetic fields and employs a feedback loop to maintain a constant, low amplitude of oscillation during sample approach and retraction. Force data are obtained from the magnetic fields required to maintain this constant amplitude. This "controlled excitation" method has important advantages when using TM-AFM methods to measure adhesion between ligands and receptors[14] or oscillatory solvation forces.[15]

Here, we focus on the use of TM-AFM to measure quasi-equilibrium steric forces between unmodified AFM tips and grafted layers of poly(ethylene glycol) (PEG). This model system was chosen since there is no appreciable adhesion between the tip and these polymer surfaces. Chains are reactively grafted to silica by conjugation to adsorbed poly(ethylenimine) (PEI) by a method that allows for control of grafting density by varying the concentration of PEG in the reaction mixture.[16,17] A key question to be addressed is whether the dynamics of polymer compression are faster than the time scale of chain escape and how this dependence may vary with grafting density.

Experimental Section

Grafting of PEG to Silica Substrates. Grafted poly(ethylene glycol) (PEG) surfaces were prepared on acid-cleaned fused silica slides (Esco Products, Oak Ridge, NJ) by reacting a succinimidyl propionic acid-derivatized PEG, MW 5000 (Nektar), with amine groups in a physisorbed high-molecular-weight branched polyethylenimine, MW 750 000 (BASF), anchoring layer. Details about the surface cleaning and grafting procedure are available elsewhere.[16,17] PEG layers of two different grafting densities were formed by using PEG adsorbing bulk concentrations of 0.1% and 2.0% (w/v) PEG in 50 mM sodium phosphate buffer, pH 7.0. From optical reflectometry, the measured surface excess concentrations of the adsorbed layers were $\Gamma = 0.3 \pm 0.1$ mg/m^2 and $\Gamma = 1 \pm 0.2$ mg/m^2, respectively,[17] corresponding to a sparsely grafted PEG layer and a densely grafted PEG layer.

AFM Force Measurements. Both DC (standard) and TM-AFM force measurements were conducted using a Nanoscope III Multimode AFM. In this particular AFM, acoustic excitation is used to induce cantilever oscillation in TM operation. Si_3N_4 cantilevers with nominal force constants (k_c) of 0.5 N/m (Veeco Metrology Group, Santa Barbara, CA) were used for both the TM-AFM and DC measurements. We chose to use these cantilevers rather than typical TM cantilevers to obtain a good signal even with sparsely covered surfaces. A driving frequency was selected at a value slightly lower than the resonant frequency. The cantilevers have a nominal resonance frequency of ~37 kHz in liquid. Exact force constants of cantilevers used were measured after completion of the experiments using the thermal noise method.[18] The accuracy of this method was substantiated through additional calibration using a reference cantilever.[19] There was good agreement between both methods in the order of magnitude of the force constant. The radii of curvature of the tips were also measured after completion of experiments by imaging a $SrTiO_3$ calibration reference[20] and were found to vary between 25 and 70 nm, with the majority being in the 25−40 nm range.

All cantilevers were cleaned by UV/ozone irradiation for 35 min before use. Force measurements were conducted in 50 mM NaCl (Debye length = 1.36 nm) to screen electrostatic interactions that arise due to the cationic polyethylenimine (PEI) anchor layer. About 100 force curves were collected at various positions on the surface, and experiments were repeated on multiple occasions to confirm reproducibility of the data. Only force curves collected during sample approach to the sample were analyzed. In our TM measurements, we focus solely on the changes in the oscillation amplitude with tip−sample separation that occur due to tip−sample forces. Phase information was not used in this analysis due to the existence of spurious resonances near to the cantilever resonance that may confound the phase signal.

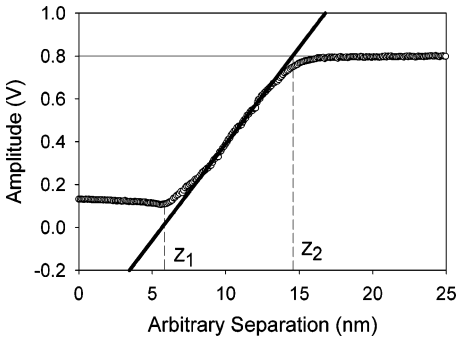

Figure 1. Detector signal (in volts) vs sample piezo position for TM-AFM on a grafted PEG layer.

Data Analysis. In DC mode, we use a standard method of calibrating the point of contact defined as the onset of a linear change in cantilever deflection with piezo movement or the constant compliance region.[21] In this region, it is assumed that the cantilever can no longer compress the sample and that all further deflection is due to the continued forced approach of the sample. In TM mode, there are two key separation distances that must be defined: (i) the instantaneous separation distance (x) and (ii) the mean separation distance (D) between the oscillating tip and sample. The tip amplitude (A) vs the relative displacements of the sample stage (Z) for a typical TM-AFM measurement is shown in Figure 1. The tip first exhibits constant-amplitude oscillation at large distances when tip−sample interactions are negligible ($Z > 18$ nm). When tip−sample interactions become significant, a decrease/increase in the tip oscillation amplitude is observed for repulsive/attractive forces, respectively. Finally, the tip returns to a constant amplitude ($Z < Z_1$). Within this final constant amplitude region, the probe's mean deflection has a sensitivity (V deflection/nm of piezo movement) that is equivalent to that obtained during constant compliance in DC measurements.[12] As such, the point of contact ($D = 0$ at $Z = Z_1$) defined this way is consistent with that of DC measurements. In measurements on polymer surfaces, it is important to recognize that this definition of $D = 0$ for either DC or TM does not necessarily correspond to absolute zero separation between the tip and the origin of the polymer attachment. We refer to D as an "apparent" separation distance to reflect this. We calibrate the cantilever amplitude (A) assuming a symmetric linear decay in amplitude will occur when the peak oscillation amplitude (A_p) is equal to the mean separation distance between the tip and incompressible sample, which may contain some trapped polymer.[22,23]

Results and Discussion

DC Compression of PEG Layers. Polymer chains grafted to a surface can have two different conformations in good solvent depending on the proximity of neighboring grafted chains. At low grafting densities, the chains will remain in a coiled structure on the surface (mushroom conformation), with the height of the polymer chains being equal to the Flory radius, R_f. As the grafting density increases with a concomitant decrease in the distance between grafted chains, polymer segments are forced to extend away from the surface in a pseudo-stretched structure known as a brush conformation. The compression of polymer mushrooms and brushes by approximately planar surfaces results in an exponential force per unit area of the general form:

$$F = Ce^{-D/\beta} \tag{1}$$

For polymer brushes, $\beta = L_b/2\pi$, and for polymer mushrooms, $\beta = R_f/2$.[24] An exponentially repulsive force of this form has also been observed in the compression of polymer brushes using sharp AFM tips.[25,26] We have previously characterized the

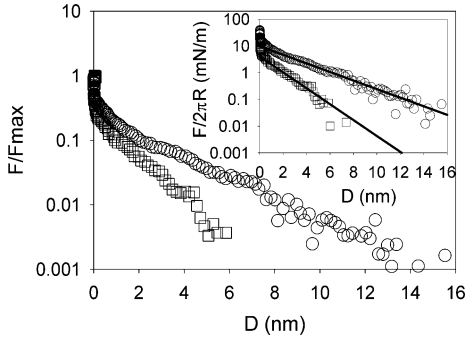

Figure 2. Force (scaled by maximum force) vs separation on sparsely grafted ($\Gamma = 0.3$ mg/m^2) PEG (□) and densely grafted grafted ($\Gamma = 1.0$ mg/m^2) PEG (○) using cantilevers of $k_c \sim 0.7$ N/m. Inset: force normalized by area of probe, equivalent to interaction energy between two flat surfaces vs apparent separation. Solid lines are exponential fits to the data: $C = 0.03$ N/m and $\beta = 1.4$ nm (□); $C = 0.06$ N/m and $\beta = 2.7$ nm (○).

Table 1. Fit Parameters for the Tip−Sample Interaction Measured on Various PEG-Coated Surfaces from Both DC and TM Force Measurements Where *C* Is the Preexponential Constant and β Is the Decay Constant (Eq 1)[a]

		DC AFM ($k_c \sim 0.5$ N/m)		TM-AFM ($k_c \sim 0.5$ N/m)	
[PEG] (mg/mL)	Γ (mg/m^2)	β (nm)	C (mN/m)	β (nm)	C (mN/m)
1	0.3 ± 0.1	1.0	0.06	1.4	0.39
1	0.3 ± 0.1	1.6	0.08	2.3	0.50
1	0.3 ± 0.1	1.4	0.03	1.0	0.39
1	0.3 ± 0.1	1.0	0.26	1.0	1.8
20	1.0 ± 0.2	2.5	0.25	2.8	1.65
20	1.0 ± 0.2	2.2	0.12	2.5	0.78
20	1.0 ± 0.2	2.7	0.06	2.9	0.40

[a] Data for TM-AFM were obtained from the best fits to eq 4 as described in the text. [PEG] is the solution concentration used during adsorption, and Γ is the surface grafting density obtained by optical reflectometry.

interfacial properties of this PEI−PEG copolymer graft using colloidal probe AFM and AFM imaging and obtained results consistent with this model.[17]

DC measurements of steric forces exerted by PEG−PEI chains in the mushroom and brush conformations using cantilevers of $k_c \sim 0.7$ N/m are shown in Figure 2. The forces have been scaled by the maximum force, experienced at $D = 0$. The onset of the steric force is about 6 nm on the PEG mushroom surface and 13 nm on the PEG brush surface. From the measured surface excess concentrations, scaling theory can be used to estimate the equilibrium height of the PEG chains in the copolymer graft:[27]

$$L_b = \Gamma^{1/3} R_f^{5/3} \tag{2}$$

From eq 2, $L_b = 6.7 \pm 0.7$ nm for the PEG mushrooms and $L_b = 10 \pm 0.7$ nm for the PEG brush. The predicted value for the PEG mushroom layer is close to reported values of R_f [6.1 nm],[28] which would be the characteristic height of the polymer in this conformation. The thickness of the PEI anchoring layer is estimated to be between 6 and 8 nm from AFM images.[17]

The forces (scaled by $2\pi R$) vs separation on both surfaces are exponential in form (see inset of Figure 2) and can be described by eq 1. Though C varies from surface to surface (Table 1), tip shape, and radius between measurements, the value of β for PEG brushes is consistently twice that for PEG mushrooms. This ratio is consistent with the difference in the onset distance of the repulsive force on the two surfaces. Variation in C is likely due to uncertainties in the measurement of cantilever spring constant.

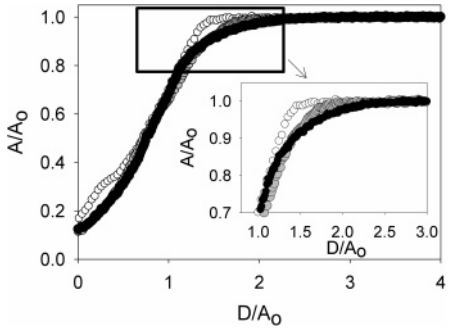

Figure 3. Normalized amplitude vs normalized separation (normalized by A_0) from TM measurements on silica (white), sparsely grafted ($\Gamma = 0.3$ mg/m^2) PEG (gray), and densely grafted ($\Gamma = 1.0$ mg/m^2) PEG (black). The inset is an enlargement of the same data highlighting the differences. A_0 is the rms tip oscillation amplitude when tip−sample interactions are negligible. Note: the small inflection near contact for the silica surface is likely due to a small jump-in owing to van der Waals interactions.

TM-AFM Compression of PEG Layers. Changes in the tip oscillation amplitude response with tip−sample interaction force are explained in established theories from frequency modulation AFM.[29] Repulsive forces increase the effective spring constant of the system by increasing the overall potential energy of the oscillator.[30] The increase in spring constant causes a positive shift in the resonance frequency of oscillation:[11]

$$\omega_{\text{eff}} = \sqrt{\frac{k_c - dF/dD}{m}} \tag{3}$$

With an increase in resonance frequency, the oscillation amplitude decreases because the oscillator is being driven at a set frequency below the oscillator's resonance frequency.[11] In contrast, attractive tip−sample interaction forces result in a decrease in the resonance frequency of oscillation and an increase in the oscillation amplitude.

The sensitivity of TM-AFM to surface composition is illustrated in Figure 3, showing amplitude vs mean separation $A(D)$ when tapping on a bare silicon substrate and the two PEG-coated surfaces of differing grafting density. At large separations, tip−sample interactions are negligible, and the tip maintains constant amplitude (free amplitude). We scale both axes by the free amplitude A_0 ($A_0 = A_{p,0}/\sqrt{2}$) to normalize the onset of sample detection for all three surfaces. Not surprisingly, the most significant amount of tip−sample repulsion (in both range and magnitude) is observed during compression of the densely grafted polymer layer (Figure 3).

At normalized distance $D/A_0 \cong 1$, the change in amplitude on all samples is equivalent and exhibits a linear decrease. On the silicon surface, the origin of the linear decay is due to hard-wall repulsion between the tip and the nondeformable silicon surface that constrains the lower bound of tip oscillation as well as frictional dissipation that occurs during tip−sample contact.[12] On the polymer-coated surfaces, this linear decay is followed by a more gradually decreasing amplitude at smaller separations ($D/A_0 < 0.5$). This gradual approach to constant amplitude is characteristic of deformation of elastomers and has been observed previously.[31]

In Figure 4, we plot the decay of the amplitude on all three surfaces for $D > A_{p,0}$. On the PEG-coated surfaces, this decay in $A(D)$ is exponential in form comparable to that observed in DC compression. Fits to the observed exponential decays using eq 1 yield values for β that are comparable to those obtained via DC compression, within the standard deviation of the

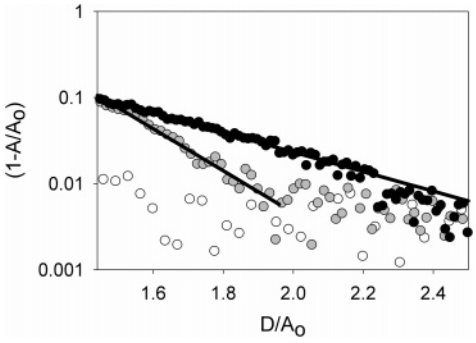

Figure 4. Normalized amplitude vs normalized separation for $D > A_{p,o}$ on silica (white); sparsely grafted PEG (gray); and densely grafted PEG (black). $A_{p,o}$ is the peak tip oscillation amplitude when tip−sample interactions are negligible.

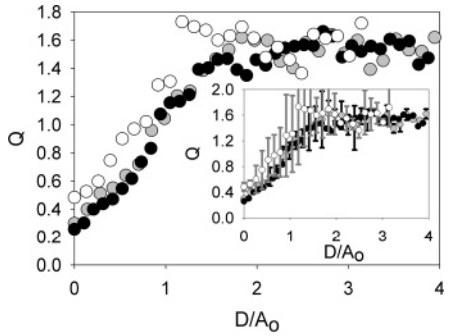

Figure 5. Energy dissipated (Q) vs normalized separation on silica (white); sparsely grafted PEG (gray); and densely grafted PEG (black). Inset: Relative error between two experiments on identical surfaces: silica (gray error bars); and sparsely grafted PEG (black error bars).

measurements (see Table 1). This indicates that ΔA has about the same distance dependence as F_{t-s}.

Quantifying the Steric Forces. To obtain a quantitative assessment of the values of C and β obtained in TM-AFM, we rely on numerical solution of the cantilever dynamics. In an earlier publication, we showed that the numerical solution of eq 4 captures the dynamics of a cantilever tapping against a silicon surface in liquid.[12] The equation of motion for the cantilever is

$$\ddot{x} + \frac{\omega_{\text{eff}}}{Q[x(t)]}\dot{x} + {\omega_{\text{eff}}}^2[x - D(t) - a_{\text{d}}\sin(\omega t)] = \frac{{\omega_{\text{eff}}}^2}{k_{\text{c}}}F_{\text{t-s}} \quad (4)$$

where ω_{eff} is the effective resonance frequency of the cantilever in liquid, Q is the quality factor, a measure of the system energy dissipation, k_{c} is the force constant of the cantilever, a_{d} is the drive amplitude, ω is the drive frequency, and $F_{\text{t-s}}$ is the tip−sample force. Using the calibration procedure outlined previously, changes in the system dissipation as a function of D [$Q(D)$] are obtained (Figure 5). Far from the surface, Q_0 is equivalent for all three surfaces within the noise of the measurement and is ∼1.5. There appears to be increased dissipation on the polymer-coated surfaces that may be due to increased viscosity within the compressed polymer layer. In the absence of a large number of sample points, we simply use a linear fit for the data $0 < D < 2A_0$. In the region of exponential amplitude attenuation before hard contact that we attribute to steric forces, we find that Q is constant and equal to Q_0.

The physical parameters characterizing the cantilever's oscillation (ω_{eff}, ω, a_{d}, k_{c}, Q) and the tip radius R are known parameters. Figure 6a,b illustrates the best fits obtained for the experimental $A(D)$ force curves varying C for the two PEG-coated surfaces. For both surfaces, the fits required a value for C that was about 6 times larger than that observed in DC compression (Table 1). Reasonable fits of the entire $A(D)$ force curves are also achieved using the calibrated form of $Q(D)$ (inset of figures). The simulation results are very sensitive to the value and onset of Q and to the decay length. The deviation in the fit on the PEG brush is due to the increased noise around $D/A_0 = 2$ that clouds the identification of the onset of Q decay (see Figure 5). This noise may be due to small perturbations of the cantilever's oscillation from hydrodynamic forces originating from limited fluid movement within the brush. We point out that it was not necessary to vary β for good fits to be obtained, and the DC AFM values for β were used for each fit, varying only C (Table 1).

A larger apparent elastic force measured in dynamic compression vs static compression has been observed by other authors. Overney[32] observed that the magnitude of the elastic modulus measured in the dynamic compression of polystyrene brushes by AFM tips was equivalent to that measured using the surface forces apparatus (SFA). Dhinojwala and Granick[33] observed a 4-fold increase in the absolute magnitude of elastic forces in dynamic vs static compression of polybutadiene−poly(vinylpyridine) diblock copolymers using the SFA. The origin of this increase in elastic force has been ascribed to various sources, including collective resistance to compression from segments outside the contact area in dynamic compression,[32] stiffening of polymer chains due to the prevention of molecular relaxation within the time scale of dynamic compression,[1,34,35] and calibration errors.[33] Another potential source of the difference in the magnitude of the steric force measured in dynamic vs static compression is increased hydrodynamic damping due to tip oscillation. We believe that the origin of the deviation is not due to the above effects but is more likely due to a difference in the ultimate sample penetration depth when using TM-AFM vs DC AFM as described below.

Effect of Oscillation Amplitude on Measured Steric Force. TM force measurements were also conducted on both surfaces using different drive amplitudes. The fitted C for the measured forces on the PEG mushrooms as a function of the cantilever's initial oscillation amplitude A_0 are shown in Figure 7. We find C steeply increases with A_0 and that at very small A_0 C becomes equivalent to that obtained during DC compression.

For the nanometer-ranged span of TM force measurements, the most significant contribution to hydrodynamic forces is from squeeze-damping forces. This force has been shown to scale with the frequency of oscillation and is proportional to D^{-1}.[33] When polymers are present on a surface, an increased squeeze-damping force has been observed that is attributed to the restricted flow of solvent within the polymer layer.[35] However, for these measurements in which the frequency of oscillation is kept fixed, lubrication forces are not expected to cause such large changes in C with the relatively small changes in A_0.

Several authors have observed changes in polymer chain dynamics with increasing compression rate. Larger forces were observed by Biggs[1] on adsorbed poly(vinylpyrrolidone) brushes and by Klein[35] on adsorbed poly(styrene) brushes, and in both cases they attribute this to the hindrance of chain relaxation at fast compression rates, resulting in increased rigidity of the polymer chains. The fastest compression time feasible in DC measurements is on the order of 10^{-2} s. In TM-AFM, the cantilevers are driven at a frequency of about 33 kHz; thus, the compression time is on the order of 10^{-5} s. Thus, it is tempting to conclude that increased rigidity of the chains provides the 6-fold larger steric force generally measured in TM experiments. However, the use of higher approach velocities (from 3 to 900

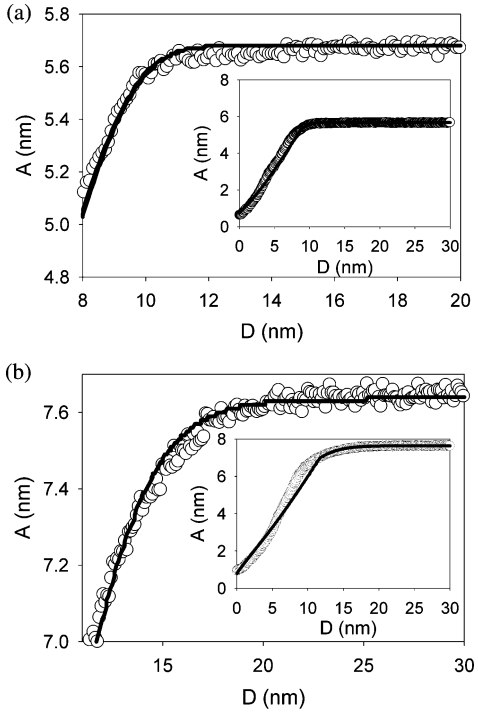

Figure 6. Experimental and simulated amplitude vs apparent separation on (a) PEG mushrooms for $D > A_{p,o}$ using the fit parameters $C = 0.39$ N/m and $\beta = 1.0$ nm; and (b) a PEG brush for $D > A_{p,o}$ using the fit parameters $C = 0.40$ N/m and $\beta = 2.9$ nm. Insets: fit of the entire force curve by including experimentally obtained $Q(D)$ in the simulation.

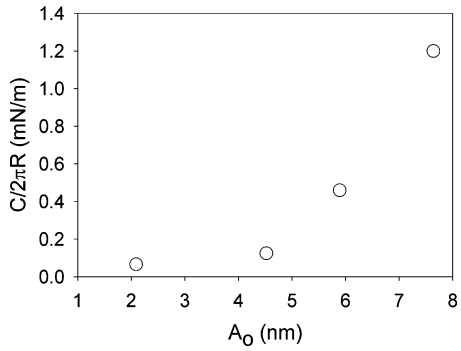

Figure 7. Magnitude of scaled preexponential term C using different initial oscillation amplitudes A_0 for TM-AFM of sparsely grafted PEG.

nm/s) in DC compression on these polymer chains did not yield larger repulsive forces in our system.

An alternative explanation for the significantly larger value of C observed in TM-AFM is a difference in the point of contact (where $D = 0$) in both measurements. Equation 1 can be modified to account for some offset in this calibrated zero separation for each measurement:

$$\frac{F}{R} = Ce^{-(D-D_0)/\beta} \tag{5}$$

By equating eq 5 to eq 1, we obtain an offset of approximately -5 nm on the PEG brush between the TM and DC measurements. This suggests that the point of constant amplitude in the $A(D)$ measurements used to calibrate $D = 0$ occurs 5 nm deeper in the copolymer graft than the point of constant compliance in the DC method. This corresponding offset is for PEG mushrooms is -3 nm.

To confirm the existence of an offset in the constant compliance states of DC and TM measurements, we obtained

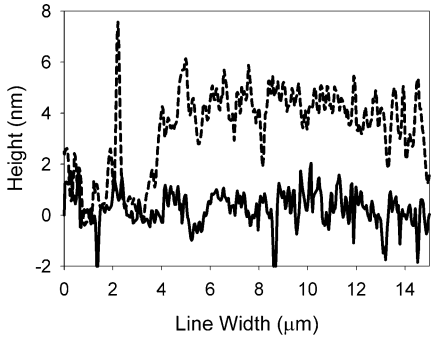

Figure 8. Vertical section of height difference between polymer-free (width < 4 μm) and PEG-grafted surfaces obtained from the contact (dashed line) and Tapping-Mode images; $A_0 = 7$ nm (solid line).

AFM images of the height difference between compressed polymer and areas on the surface absent of polymer (polymer removed by scratching gently using a 1 μm needle in a profilometer apparatus). The images were collected at loads equivalent to constant compliance in the two methods for both surfaces. Figure 8 plots two sections of those images. As expected, the compressed polymer thickness at DC constant compliance is higher than that obtained by TM-AFM with an offset of 4.4 nm, comparable to the offset calculated using eq 5. A height difference of 3.1 nm was observed on the PEG mushroom surface in accordance with the calculations. In the case of TM-AFM, as the initial oscillation amplitude of the cantilever is decreased, the observed height difference between polymer-covered and bare surfaces increases. We point out that the interaction between the tip and the PEG surfaces is nonadhesive and very weak for the bare tip and bare silica, and therefore height artifacts from differences in adhesion are not deemed significant. Similar results were observed by Knoll et al., who showed that significant indentation of the tip into spin-cast poly(styrene-*block*-butadiene-*block*-styrene) films occurs during TM measurements in air. [23] They further found that the indentation depth increased systematically with increased initial tip oscillation amplitude, A_0. We reason that the offset in the calibrated $D = 0$ between our TM and DC measurements is due to further compression/penetration in TM of the putative incompressible layer in DC compression. On the basis of this reasoning, at $A_0 = 2$ nm (Figure 7), the tip does not have enough momentum to compress/penetrate the incompressible layer, and the obtained C is comparable to that obtained from DC compression.

The results in Table 1 demonstrate that the quasi-equilibrium steric forces measured DC AFM match those measured using TM-AFM for PEG layers with nonoverlapping chains and stretched chains. The discrepancy in the value of C is explained by differences in the high-load point of contact for the two methods, and the values for β are comparable. While we cannot be sure that escape transitions do not occur in any of these systems, their presence tends to decrease the magnitude of steric forces. C was uniformly larger for TM-AFM over DC AFM for both mushroom and brush layers, even though escape events are believed to be suppressed by the strong lateral interactions in polymer brushes. We conclude that both methods reveal about the same polymer steric forces, despite the much faster time scales and deeper ultimate penetration of TM-AFM.

Conclusions

Amplitude vs distance curves obtained while probing grated PEG layers show characteristic features that reflect the grafting density and thickness of the layers. More quantitative informa-

tion can be obtained by modeling the cantilever dynamics to account for distance-dependent damping, revealing the tip−sample force. This showed that conventional DC AFM and TM-AFM methods produce about the same force−distance data for grafted PEG layers in aqueous solution, regardless of whether the layers were in the stretched or nonoverlapping conformations. Care must be taken to account for differences in the point of contact for each method. After accounting for the higher ultimate penetration of the AFM tip when using TM-AFM, both the magnitude and the decay constant for the exponentially increasing steric forces were comparable. While this work focused on fitting model parameters that describe steric stabilization forces, it should be possible to obtain the full force profile for an unknown sample by a similar approach.

Acknowledgment. The authors acknowledge the ACS Petroleum Research Fund (#37734-G7) and the National Science Foundation (CTS-0210205) for financial support of this work.

References and Notes

(1) Biggs, S. *Langmuir* **1995**, *11*, 156−162.
(2) Kelley, T. W.; Schorr, P. A.; Johnson, K. D.; Tirrell, M.; Frisbie, C. D. *Macromolecules* **1998**, *31*, 4297−4300.
(3) Braithwaite, G. J. C.; Luckham, P. F. *J. Colloid Interface Sci.* **1999**, *218*, 97−111.
(4) Yamamoto, S.; Ejaz, M.; Tsujii, Y.; Matsumoto, M.; Fukuda, T. *Macromolecules* **2000**, *33*, 5602−5607.
(5) Ducker, W. A.; Senden, T. J.; Pashley, R. M. *Nature (London)* **1991**, *353*, 239−241.
(6) Larson, I.; Drummond, C. J.; Chan, D. Y. C.; Grieser, F. *J. Am. Chem. Soc.* **1993**, *115*, 11885.
(7) Braithwaite, G. J. C.; Howe, A.; Luckham, P. F. *Langmuir* **1996**, *12*, 4224−4237.
(8) Hartley, P. G.; Scales, P. J. *Langmuir* **1998**, *14*, 6948−6955.
(9) Murat, M.; Grest, G. *Macromolecules* **1996**, *29*, 8282−8284.
(10) Guffond, M. C.; Williams, D. R. M.; Sevick, E. M. *Langmuir* **1997**, *13*, 5691−5696.
(11) García, R.; Pérez, R. *Surf. Sci. Rep.* **2002**, *47*, 197−301.
(12) Nnebe, I.; Schneider, J. W. *Langmuir* **2004**, *20*, 3195−3201.
(13) Sader, J. E.; Uchihashi, T.; Higgins, M. J.; Farrell, A.; Nakayama, Y.; Jarvis, S. P. *Nanotechnology* **2005**, *16*, S94−S101.
(14) Higgins, M. J.; Riener, C. K.; Uchihashi, T.; Sader, J. E.; McKendry, R.; Jarvis, S. P. *Nanotechnology* **2005**, *16*, S85−S89.
(15) Uchihashi, T.; Higgins, M. J.; Yasuda, S.; Jarvis, S. P.; Akita, S.; Nakayama, Y.; Sader, J. E. *Appl. Phys. Lett.* **2004**, *85*, 3575−3577.
(16) Brink, C.; Österberg, E.; Holmberg, K.; Tiberg, F. *Colloids Surf.* **1992**, *66*, 149−156.
(17) Nnebe, I. M.; Tilton, R. D.; Schneider, J. W. *J. Colloid Interface Sci.* **2004**, *276*, 306−316.
(18) Hutter, J. L.; Bechhoefer, J. *Rev. Sci. Instrum.* **1993**, *64*, 1868−1873.
(19) Tortonese, M.; Kirk, M. *Proc. SPIE* **1997**, *3009*, 53−60.
(20) Sheiko, S. S.; Möller, M.; Reuvekamp, E.; Zandbergen, H. W. *Phys. Rev. B* **1993**, *48*, 5675−5678.
(21) Ducker, W. A.; Senden, T. J. *Langmuir* **1992**, *8*, 1831−1836.
(22) Lantz, M.; Liu, Y. Z.; Cui, X. D.; Tokumoto, H.; Lindsay, S. M. *Surf. Interface Anal.* **1999**, *27*, 354−360.
(23) Knoll, A.; Magerle, R.; Krausch, G. *Macromolecules* **2001**, *34*, 4159−4165.
(24) Israelachvili, J. *Intermolecular and Surface Forces*; Academic Press: New York, 1992.
(25) O'Shea, S. J.; Welland, M. E.; Rayment, T. *Langmuir* **1993**, *9*, 1826−1835.
(26) Butt, H.-J.; Kappl, M.; Mueller, H.; Raiteri, R. *Langmuir* **1999**, *15*, 2559−2565.
(27) de Gennes, P. G. *Adv. Colloid Interface Sci.* **1987**, *27*, 189−209.
(28) Rex, S.; Zuckermann, M.; Lafleur, M.; Silvius, J. R. *Biophys. J.* **1998**, *75*, 2900−2914.
(29) Giessibl, F. J.; Bielefeldt, H. *Phys. Rev. B* **2000**, *61*, 9968−9971.
(30) Hölscher, H.; Schwarz, U. D.; Wiesendanger, R. *Appl. Surf. Sci.* **1999**, *140*, 344−351.
(31) Bar, G.; Delineau, L.; Brandsch, R.; Ganter, M.; Whangbo, M.-H. *Surf. Sci.* **2000**, *457*, L404−L412.
(32) Overney, R. M.; Leta, D. P.; Pictroski, C. F.; Rafailovich, M. H.; Liu, Y.; Quinn, J.; Sokolov, J.; Eisenberg, A.; Overney, G. *Phys. Rev. Lett.* **1996**, *76*, 1272−1275.
(33) Dhinojwala, A.; Granick, S. *Macromolecules* **1997**, *30*, 1079−1085.
(34) Biggs, S.; Proud, A. D. *Langmuir* **1997**, *13*, 7202−7210.
(35) Klein, J.; Kamiyama, Y.; Yoshizawa, H.; Israelachvili, J. N.; Fredrickson, G. H.; Pincus, P.; Fetters, L. J. *Macromolecules* **1993**, *26*, 5552−5560.

MA050045Q